THYROID
Volume 19, Number 8, 2009

DOI: 10.1089/thy.2008.0362

Distinct Genetic Alterations in the Mitogen-Activated Protein Kinase Pathway Dictate Sensitivity of Thyroid Cancer Cells to Mitogen-Activated Protein Kinase Kinase 1/2 Inhibition

Rebecca E. Schweppe, Anna A. Kerege, Vibha Sharma, Joanna M. Poczobutt, Arthur Gutierrez-Hartmann, Rachel L. Grzywa, and Bryan R. Haugen

Background: The mitogen-activated protein kinase (MAPK)/extracellular signal–regulated kinase (ERK) pathway plays an important role in papillary and anaplastic thyroid cancer (PTC and ATC) due to activating mutations in *BRAF*, RAS, or rearrangements in RET/PTC1. The objective of this study was to thoroughly test whether the *BRAF* V600E mutation predicts response to mitogen-activated protein kinase kinase 1/2 (MKK1/2) inhibition, as shown in other tumor types, using an authenticated panel of thyroid cancer cell lines.
Methods: PTC and ATC cells harboring distinct mutations in the MAPK pathway were treated with two different inhibitors selective for MKK1/2 (CI-1040 or U0126). The consequences of MKK1/2 inhibition on cell growth, survival, invasion, and MAPK signaling was determined.
Results: Inhibition of MKK1/2 using CI-1040 or U0126 differentially inhibits the growth of a panel of PTC and ATC cell lines in two-dimensional culture, with those harboring the *BRAF* V600E mutation (SW1736) or *BRAF*-V600E/PI3K-E542K mutations (K1) being the most sensitive, the RET/PTC1 rearrangement (TPC1) and *BRAF* V600E mutant (BCPAP), intermediate, and the HRAS-G13R mutant (C643), the least sensitive. Growth of these cells is more sensitive to MKK1/2 inhibition when grown in 2% versus 10% serum. Baseline levels of phospho-ERK1/2 were similar in all of the cell lines, and inhibition phospho-ERK1/2 did not predict sensitivity to MKK1/2 inhibition. When cells are grown in three-dimensional culture, MKK1/2 inhibition of growth correlates with mutational status (*BRAF* > RET/PTC1 > RAS). Finally, PTC and ATC invasiveness is differentially inhibited by CI-1040, which is independent of tumor type or mutation present.
Conclusions: Different mutations in the MAPK pathway play distinct roles in the growth and invasion of thyroid cancer cells. These results indicate that MKK1/2 inhibitors have the potential to inhibit thyroid cancer growth and invasion, but that responses differ based on mutation status and growth conditions.

Introduction

Deregulation of the mitogen-activated protein kinase (MAPK)/extracellular signal–regulated kinase (ERK) pathway plays an important role in many types of cancer. The MAPK/ERK pathway consists of a three-tiered kinase cascade that proceeds via sequential activation and phosphorylation of the mitogen-activated protein kinase kinase (MKK) Raf, MKK1/2, and ERK1/2. In normal cells, the MAPK/ERK pathway is typically activated by mitogens and growth factors, which results in the regulation of a variety of cellular processes, including growth, differentiation, apoptosis, and survival. In cancer, the MAPK pathway is commonly activated by overexpression, amplification, or mutation of upstream signaling components. A valine to glutamate (V600E) mutation in *BRAF* is one of the most common genetic lesions in human cancer that leads to constitutive activation of the MAPK pathway (1), as are mutations among Ras family members and upstream tyrosine kinase receptors, such as epidermal growth factor receptor (*EGFR*) (2). Given the importance of the MAPK/ERK pathway in cancer, components of this pathway represent attractive therapeutic targets, and inhibitors targeting MKK1/2 and Raf are being studied intensively and are currently in clinical trials (3).

Recent studies have indicated that the presence of the *BRAF* V600E mutation renders cancer cells more susceptible to MKK1/2 inhibition when compared to cells where the MAPK pathway is constitutively active due to other upstream activating events, such as mutations in the *EGFR* or Ras family members (4–7). These observations are consistent with the idea that *BRAF* specifically activates MKK1/2, whereas other upstream signaling components (i.e., *EGFR* or Ras) activate

Division of Endocrinology, Diabetes, and Metabolism, University of Colorado Denver, Aurora, Colorado.

additional pathways, and are therefore less dependent on MKK1/2 (4). Although several studies have shown that the *BRAF* mutation predicts sensitivity to MKK1/2 inhibition, other studies have shown no correlation (8–10). The basis for these conflicting results is not known, although extracellular growth factors may play an important role (11,12). These conflicting results suggest that patient therapy should not necessarily be directed by the presence or absence of the *BRAF* V600E mutation.

Aberrant activation of the MAPK pathway plays an important role in papillary and anaplastic thyroid cancer (PTC and ATC) (13,14). PTC is the most common endocrine malignancy. The prognosis for many patients with differentiated thyroid cancer is excellent, but a significant minority of patients (10–20%) do not respond to standard therapies (15). ATC is less common and it is one of the most aggressive human cancers with greater than 95% mortality at 6 months. The MAPK pathway is constitutively active in the majority of PTCs (70%) due to upstream activating mutations in *BRAF*, RET/PTC, RAS or NTRK, with genetic alterations in *BRAF* (V600E) and RET/PTC being the most common genetic events (45% and 20–40%, respectively), and RAS mutations occurring less frequently (16,17). The *BRAF* V600E mutation is less common in ATC (10–35%) (18,19), and the prevalence of RAS mutations is higher in ATC compared to PTC (20). Like most cancers, these mutations are generally thought to be mutually exclusive, demonstrating the importance of the MAPK/ERK pathway in PTC and ATC.

Inhibition of the MAPK pathway in PTC using *BRAF* siRNA or pharmacological inhibition of *BRAF*, MKK1/2, or RET/PTC results in cell cycle arrest *in vitro* and blocks tumor growth in xenograft mouse models, making the MAPK pathway an attractive pharmacologic target in thyroid cancer (5,7,21–24). Despite the importance of *BRAF* and RET/PTC signaling in PTC tumorigenesis, clinical studies have shown that single-agent inhibitors of the MAPK pathway are not sufficient to induce a complete response (25). Thus, further studies are needed to characterize MKK1/2 inhibitor sensitivity of thyroid cancer cells.

To further study the role of MKK1/2 in thyroid cancer, we examined the effects of two selective MKK1/2 inhibitors (CI-1040 and U0126) on a panel of authenticated PTC and ATC cell lines harboring different genetic alterations in the MAPK pathway using two-dimensional (2D) and three-dimensional (3D) cell culture approaches. Our results show that different genetic alterations in the MAPK pathway serve important, yet distinct, roles in thyroid cancer cells, but that other pathways are likely involved.

Materials and Methods

Cell culture

Human thyroid carcinoma cell lines used in this study are listed in Table 1. The C643 and SW1736 cells were kindly provided by Dr. K. Ain with permission from Dr. N.-E. Heldin (University Hospital, S-751 85 Uppsala, Sweden). The TPC1 cells were kindly provided by Dr. S. Jhiang (Ohio State University, Columbus, OH), the BCPAP cells were kindly provided by Dr. M. Santoro (Medical School, University "Federico II" of Naples, Naples, Italy), and the K1 cells were kindly provided by Dr. Wynford-Thomas (Cardiff University, Cardiff, United Kingdom). The cell lines used in this study were analyzed by short tandem repeat profiling and shown to be unique (26). Cells were grown in RPMI (Invitrogen, Carlsbad, CA) containing 2% or 10% FBS (HyClone Laboratories, Logan, UT) and maintained at 37°C in 5% CO_2.

MKK1/2 inhibitors

The MKK1/2 inhibitors U0126 (Calbiochem, Gibbstown, NJ) and CI-1040 (Pfizer, Ann Arbor, MI) were dissolved in DMSO at 10 mM.

Western blot analysis

Cells were harvested at 80–85% confluency at the indicated time points in extraction buffer containing 1% Triton X-100, 10 mM Tris, pH 7.4, 5 mM EDTA, 50 mM NaCl, 50 mM NaF, 1 mM phenylmethylsulfonyl fluoride, and 2 mM Na_3VO_4 supplemented with 1× complete protease inhibitors (Roche Diagnostics, Indianapolis, IN). For the PARP cleavage analysis, cells in the medium were collected from each plate, rinsed 1× with phosphate buffered saline (PBS), and combined with the remaining adherent cells in extraction buffer. Protein concentrations were determined using the Bio-Rad DC protein assay (Bio-Rad Laboratories, Hercules, CA), and cell extracts (30 μg) were separated on 10% polyacrylamide (PAGE)–SDS gels, and transferred to Immobilon-P membranes (Millipore, Bedford, MA). Membranes were incubated with primary antibodies recognizing phospho-ERK1/2 (ppERK1/2) (Thr202/Tyr204; Cell Signaling, Danvers, MA), ERK2 (C14 ERK2; Santa Cruz, Santa Cruz, CA), ppMKK1/2 (S218/S222; Cell Signaling), MKK1/2 (Cell Signaling), or cleaved PARP Asp 214 (Clone F21-852; BD Biosciences, San Jose, CA) in blocking buffer containing 5% milk in 20 mM Tris pH 7.4, 138 mM NaCl, and 0.1% Tween (TBST). Blots containing ppMKK1/2 antibody were incubated in TBST con-

Table 1. Summary of Mitogen-Activated Protein Kinase Kinase 1/2 Inhibition of Human Thyroid Cancer Cell Lines

Cell line	*C643*	*TPC1*	*BCPAP*	*SW1736*	*K1*
Mutation	*HRAS G13R*	*RET/PTC1*	BRAF *V600E*	BRAF *V600E*	BRAF *V600E/PI3K E542K*
Tumor Type	*ATC*	*PTC*	*PTC*	*ATC*	*PTC*
ViCell CI-1040 IC50	0.76	0.69	0.55	0.23	0.07
ViCell CI-1040	21%	54%	51%	81%	87%
ViCell U0126	32%	38%	55%	73%	86%
3D CI-1040	28%	55%	88%	83%	79%
Invasion	12%	81%	55%	20%	18%

Cells grown in the medium supplemented with 10% FBS. IC50 values (μM) for CI-1040 or % inhibition by CI-1040 or U0126 are shown. ATC, anaplastic thyroid cancer; PTC, papillary thyroid cancer; 3D, three-dimensional.

taining 3% bovine serum albumin or 5% ECL advance blocking buffer (GE Healthcare, Piscataway, NJ). Membranes were washed with TBST and incubated with secondary donkey anti-rabbit or sheep anti-mouse horseradish peroxidase–conjugated antibody (GE Healthcare). Antigen–antibody complexes were viewed by enhanced chemiluminescence detection (SuperSignal West Pico; Pierce, Rockford, IL) or ECL Advance (GE Healthcare), where indicated. Blots were stripped and reprobed, where indicated, using Re-Blot Plus Mild (Millipore).

ViCell counting

Cells were plated in duplicate in 6-cm dishes in RPMI containing 10% or 2% FBS, where indicated, at 7500 cells/dish for the TPC1 cells, and at 15,000 cells/dish for the remaining cells. The medium containing 3 μM U0126, 0.5 μM CI-1040, or DMSO was replaced every 3 days for 6 days. Cells in the medium were collected, and adherent cells were harvested using trypsin–EDTA at 6 days, quenched with RPMI containing 10% or 2% serum, and resuspended in 1 mL PBS. Viable cells were counted using the Beckman Coulter ViCell cell counter at the University of Colorado Cancer Center Flow Cytometry Core, which counts 100 fields of cells and calculates viable cells using trypan blue exclusion. For IC50 calculations, the percent viable cells/mL was plotted versus the log of CI-1040 concentration, and nonlinear regression with a slope sigmoidal dose–response curve was generated along with IC_{50} using GraphPad Prism software (GraphPad Software, San Diego, CA).

Cellular proliferation assays

Cells (500/well for TPC1 and C643, and 1000/well for BCPAP, SW1736, K1, NPA87, DRO90, and ARO81) were seeded in quadruplicate in 96-well plates in RPMI containing 2% or 10% FBS, as indicated. Cells were treated the next day with the medium containing 3 μM U0126, 0.5 μM CI-1040, or DMSO, and the fresh medium containing the indicated drug was replenished every 3 days, as described above. Cells were assayed at 3- and 6-day time points, and proliferation was measured following the manufacturer's instructions using the CellTiter 96 Aqueous Non-Radioactive Cell Proliferation Assay (Promega, Madison, WI), as previously described (27). Each plate was read using the MRX Microplate Reader (Dynatech Laboratories, Chantilly, VA) and the Revelation software at an absorbance of 490 nm.

Cell cycle analysis

Cells were plated in 6-cm dishes at 0.5×10^5/well (TPC1) or 1×10^5/well (C643, BCPAP, SW1736, and K1), and treated with 0.5 μM CI-1040 or vehicle (DMSO) in RPMI containing 10% FBS. Cells were collected by trypsinization at 48 hours and washed twice in ice-cold PBS. Cell pellets were resuspended in a saponin/propidium iodide solution (0.3% saponin, 25 μg/mL propidium iodide, 0.1 mM EDTA, and 10 μg/mL RNase A). Cells were incubated at 4°C for 24 hours, and cell cycle distribution was determined by flow cytometry using a Beckman Coulter FC500 at the University of Colorado Cancer Center Flow Cytometry Core. ModFit LT (Verity Software House, Topsham, ME) was used for cell cycle modeling and doublet discrimination.

Invasion assays

Cells were treated for 18 hours in the presence of 0.5 μM CI-1040 or vehicle (DMSO) in RPMI containing 0.1% FBS. Cells (10^5) were plated in the upper chambers of Matrigel-coated transwell chambers (24-well, 8 μM pore size; BD Biosciences) in RPMI supplemented with 0.1% FBS in the presence or absence of CI-1040 (0.5 μM). Cells were allowed to invade toward RPMI containing 2% FBS with or without CI-1040 (0.5 μM). After 24 hours, noninvading cells on the top chamber were removed by scraping with a cotton swab, and invading cells on the lower surface were fixed with methanol and stained with 3 μg/mL 4′,6-diamidino-2-phenylindole (DAPI; Invitrogen). Invading cells were measured by counting DAPI-stained nuclei in five microscopic fields under 10× magnification using the Metamorph software attached to a Nikon microscope. Images of noninvading cells were also analyzed in parallel to ensure equal plating. Results shown are the mean ± standard error of mean of three independent experiments.

3D culture

Spheroids were formed using the Matrigel overlay method, as previously described (28). Briefly, 5000 cells were plated in 8-well chamber slides (BD Biosciences) on growth factor–reduced Matrigel (BD Biosciences), in a 2% Matrigel solution in RPMI supplemented with 10% FBS. After 4 days of growth, spheroids were established, and the medium containing 0.5 μM CI-1040 or DMSO was added and replaced every 4 days for 8 additional days. Cells were fixed in 2% paraformaldehyde and processed for immunoflourescence according to a published protocol. Briefly, cells were stained with the anti-Ki67 antibody (1:50 dilution; Zymed, South San Francisco, CA), followed by incubation with a goat anti-rabbit Alexa Fluor-594–conjugated secondary antibody (1:200 dilution; Invitrogen #A-11037) and counterstained with 100 ng/mL DAPI (Invitrogen). Cells were incubated with a goat anti-mouse Alexa–conjugated secondary antibody (1:200 dilution; Invitrogen). Images were collected using a confocal light microscope (Olympus Spinning Disk, Center Valley, PA) in the UCD Light Microscopy Facility. Growth inhibition was quantitated by measuring the area $(\mu m)^2$ of spheroids in four different fields (4× magnification; Image J) for the TPC1, BCPAP, SW1736, and K1 cells. Growth inhibition of the C643 cells was quantitated by calculating the average number of DAPI-positive pixels/area in 5–7 different fields, since these cells formed branching networks rather than masses in 3D culture, and it was not possible to calculate the area by diameter measurements. Results presented are the mean ± standard error of mean of two replicates from one independent experiment.

Results

MKK1/2 inhibition differentially inhibits PTC and ATC cell growth by ViCell counting

The growth of a panel of five PTC and ATC cells harboring the HRAS G13R mutation (C643), RET/PTC1 rearrangement (TPC1), *BRAF* V600E mutation (BCPAP, SW1736), or *BRAF* V600E and PI3K E542K (K1) in response to MKK1/2 inhibition was evaluated by ViCell counting. Concentrations of CI-1040 (0.5 μM) and U0126 (3 μM) were used, which selectively

inhibit MKK1/2 but not other kinases, including the related MKK5 (29). Figure 1A shows that CI-1040 or U0126 treatment of cells grown in the medium supplemented with 10% serum resulted in a significant inhibition of growth of all cell lines tested. The Ras-mutant C643 cell line was the least sensitive to CI-1040 or U0126 treatment (20% and 32% inhibition, respectively), and the TPC1 (RET/PTC1) and *BRAF*-mutant BCPAP cells were similarly inhibited (Fig. 1A, Table 1; 37–55% inhibition). The growth of the *BRAF*-mutant SW1736 was effectively inhibited by CI-1040 or U0126 treatment (81% and 74% inhibition, respectively). The *BRAF*/PI3K-mutant K1 cells were the most sensitive to MKK1/2 inhibition by ViCell counting (Fig. 1A; ~85% inhibition). The differential sensitivity of growth inhibition is likely not due to drug stability, as similar results were observed when cells were treated with CI-1040 or U0126 on a daily basis (data not shown). Dose response with CI-1040 revealed that the IC50 for the C643, TPC1, and BCPAP cells was similar (0.76 ± 0.13, 0.69 ± 0.09, and $0.55 \pm 0.09\ \mu$M, respectively), indicating that these cell lines are similarly susceptible to CI-1040 treatment despite harboring distinct mutations in the MAPK pathway (RAS vs. RET/PTC1 vs. *BRAF* V600E) (Table 1).

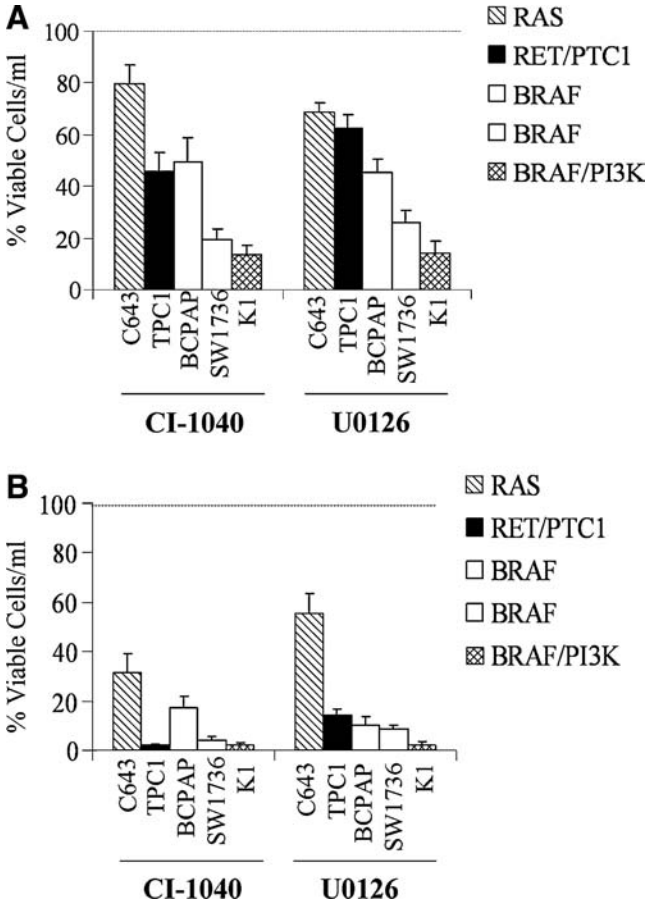

FIG. 1. Inhibition of cell growth of thyroid cancer cells by CI-1040 or U0126. Cells (C643, TPC1, BCPAP, SW1736, and K1) were grown in RPMI supplemented with 10% FBS (**A**) or 2% FBS (**B**) and treated with or without CI-1040 (0.5 μM) every 3 days for 6 days as described in the Materials and Methods. Viable cells/mL was measured using the Vi-Cell Coulter Counter (Beckman). Vehicle/control was set to 100% and is represented by the dashed line. Results presented are the mean ± SD of three experiments done in duplicate. Statistical analysis (two-tailed *t*-test) of cells grown in 10% FBS indicated that the C643 ($p = 0.04$), TPC1 ($p = 0.006$), BCPAP ($p = 0.01$), SW1736, and K1 ($p = 0.001$) were significantly inhibited by CI-1040 treatment, and that the C643 ($p = 0.004$), TPC1 ($p < 0.006$), BCPAP ($p = 0.003$), SW1736, and K1 ($p = 0.001$) were significantly inhibited by U0126 treatment.

Activation of the MAPK pathway typically occurs through upstream activation of growth factor receptor signaling, which can occur when cells are grown in the medium containing higher levels of serum. We therefore investigated the potential role of growth factors present in serum that could affect MKK1/2 inhibitor sensitivity. For these studies, PTC and ATC cells were grown in RPMI containing 2% FBS, and the effect of CI-1040 and U0126 on the growth of these cells was evaluated by ViCell counting, as described above. Under these conditions, the growth of all cell lines was effectively inhibited by CI-1040 or U0126 (Fig. 1B). Although the Ras-mutant C643 cell line was the least affected, a growth inhibition of 40–65% was achieved with CI-1040 or U0126 (Fig. 1B). The more profound inhibition of growth in low serum indicates that growth factors and/or mitogens, in addition to proto-oncogene–mediated signaling, play an important role in the growth of PTC and ATC cells (Fig. 1).

As shown in Figure 1, CI-1040 or U0126 treatment resulted in a significant inhibition of proliferation of all cell lines regardless of mutational status. Interestingly, when proliferation was measured using the MTS assay, inhibition of MKK1/2 with CI-1040 or U0126 was less effective when cells were grown in the medium supplemented with 2% or 10% serum, with the exception of the SW1736 cells that were the most sensitive (Supplemental Fig. S1, available online at www.liebertonline.com). Interestingly, the K1 cells exhibited a paradoxical increased proliferation in response to CI-1040 and U0126 at 3 days when grown in 2% FBS (Supplemental Fig. S1, ~2-fold), and this response was attenuated after 6 days of treatment (Supplemental Fig. S1, 30–40% inhibition). Thus, despite the presence of constitutive MAPK signaling in these cell lines, proliferation is modestly affected by MKK1/2 inhibitors using the MTS assay.

MKK1/2 regulation of the cell cycle

To determine the mechanism by which CI-1040 and U0126 treatment results in reduced cell numbers (Fig. 1), the effect of MKK1/2 inhibition on cell cycle progression was evaluated. For these studies, CI-1040 was used to inhibit the MAPK pathway due to its higher potency. Figure 2 shows the cell cycle distribution of the thyroid cancer cell lines in response to CI-1040 treatment for 48 hours. The cell cycle profile of the Ras-mutant C643 cell line was not significantly affected by CI-1040 treatment (Fig. 2). In contrast, a significant decrease in the fraction of S-phase cells with a concomitant increase in G1-phase cells was observed in the RET/PTC1-expressing TPC1 cells and *BRAF*-mutant SW1736 cells in the presence of CI-1040. The *BRAF*-mutant BCPAP and *BRAF*/PI3K-mutant K1 cells also exhibited an increase in the proportion of cells in G1 and a decrease of cells in S phase in the presence of CI-1040; however, this did not reach statistical significance (Fig. 2). No sub-G1 peak was observed in any of the cell lines, indicating that the reduction in cell number in response to

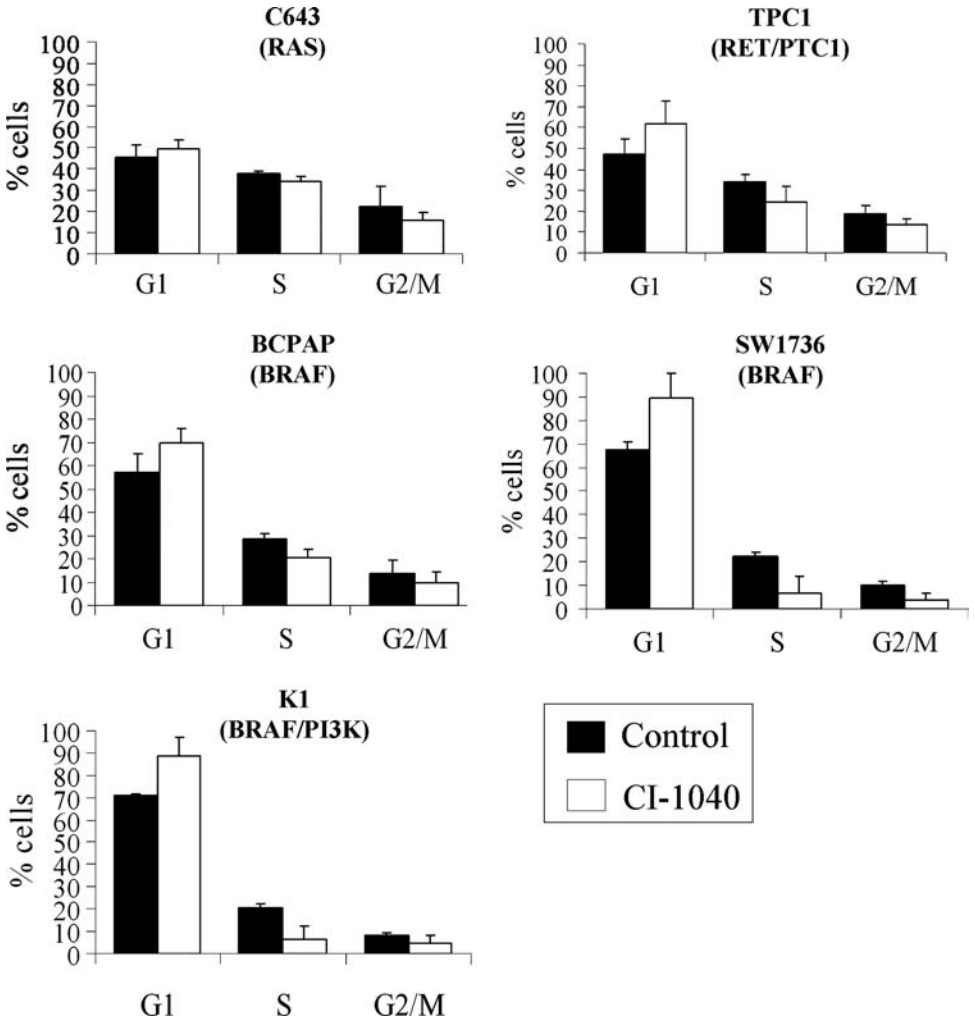

FIG. 2. Inhibition of cell cycle progression in response to CI-1040 treatment. Cells were grown in RPMI supplemented with 10% FBS and treated with or without 0.5 μM CI-1040 for 48 hours. After 48 hours, cells were collected and stained in a saponin/propidium iodide solution and subjected to FACS analysis to evaluate cell cycle distribution. Statistical analysis (two-tailed *t*-test) indicated that the proportion of TPC1 ($p = 0.02$) and SW1736 ($p = 0.03$) was significantly increased at G1 in the presence of CI-1040, while cell cycle distribution of the C643 cells ($p = 0.3$) was not significantly inhibited. The proportion of cells in G1 was increased in the presence of CI-1040 for the BCPAP ($p = 0.06$) and K1 cells ($p = 0.08$) but did reach statistical significance.

MKK1/2 inhibition is due to growth inhibition rather than apoptosis (data not shown).

To confirm the effect of MKK1/2 inhibition on cell cycle progression rather than apoptosis, cleavage of the caspase substrate, poly(ADP-ribose) polymerase 1 (PARP1), in response to MKK1/2 inhibition was monitored by Western blot analysis using an antibody that specifically recognizes the cleaved form (30). For these studies, cells were treated with or without CI-1040 (0.5 μM) for 24 hours and both floating and adherent cells were harvested. As shown in Figure 3, the appearance of the 85 kDa cleaved form of PARP was observed in the presence of CI-1040 in the DRO90 melanoma cell line, which was used as a positive control in these studies. MKK1/2 inhibition by CI-1040 resulted in low levels of the 85 kDa fragment in the C643, BCPAP, and SW1736 cell lines and low to undetectable levels in the K1 and TPC1 cell lines, suggesting minimal induction of apoptosis by the MKK1/2 inhibitor in thyroid cancer cell lines (Fig. 3).

Correlation of ppERK1/2 and ppMKK1/2 levels with growth inhibition

To determine whether the differential sensitivity of growth in response to MKK1/2 inhibition (Fig. 1) is due to differential MAPK pathway activation, basal levels of ppERK1/2 were measured by Western blot analysis. Figure 4 shows that Control (C) ppERK1/2 and total ERK2 levels are similar in the panel of cell lines, independent of oncogene mutational status, tumor classification, response to treatment, or serum concentration. Selective inhibition of MKK1/2 with CI-1040 or U0126 rapidly blocks ppERK1/2 at 4 hours, and ppERK1/2 levels variably recover by 24–48 hours independent of oncogene status, tumor type, or growth conditions (Fig. 4A, B). Inhibition of ppERK1/2 with CI-1040 or U0126 did not correlate with inhibition of growth (Fig. 1). To determine whether recovery of ppERK1/2 levels was due to drug stability, cells treated with CI-1040 for 48 hours were re-treated with or without CI-1040 for the last 4 hours. In some cases ppERK1/2 levels were reduced by redosing with CI-1040 for the last 4 hours (C643, BCPAP, and K1), but overall, ppERK1/2 levels did not correlate with growth inhibition (data not shown).

Next we assessed whether ppMKK1/2 levels predict response to growth inhibition by CI-1040 or U0126. Figure 4A and B shows that under basal conditions, ppMKK1/2 levels are low to undetectable in the C643 and TPC1 cells grown in the medium supplemented with 10% and 2% serum, and in the SW1736 cell line grown in the medium supplemented with 2% serum. Treatment with CI-1040, but not U0126, results in a

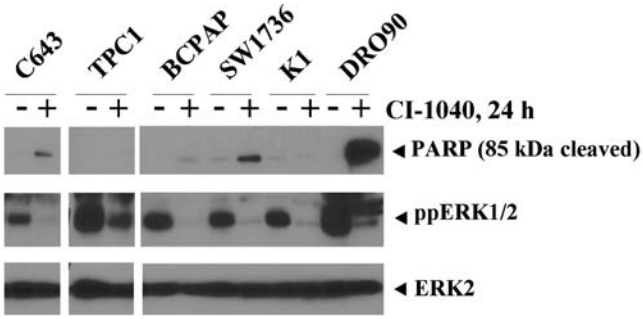

FIG. 3. Analysis of PARP cleavage in response to MKK1/2 inhibition. Cells were grown in RPMI supplemented with 2% FBS and treated with or without 0.5 μM CI-1040 for 24 hours, as indicated. Whole cell extracts (30 μg) were separated by 10% PAGE-SDS, and PARP cleavage was monitored by Western blot analysis with an antibody that specifically recognizes cleaved PARP (top panel, 85 kDa cleaved). Expression and inhibition of ppERK1/2 and ERK2 was analyzed in parallel, as described in Figure 4. Similar results were obtained in 2–3 additional experiments. MKK1/2, mitogen-activated protein kinase kinase 1/2; ERK, extracellular signal–regulated kinase; ppERK1/2, phospho-ERK1/2.

paradoxical increase in ppMKK1/2 levels in these cells at all time points examined (Fig. 4). Low levels of ppMKK1/2 in the TPC1 and C643 cells are consistent with previous studies (7,31). Despite the increase in ppMKK1/2 with CI-1040 treatment, the MAPK pathway is effectively inhibited as demonstrated by the inhibition of ppERK1/2 (Fig. 4) and phospho-p90RSK (data not shown). Elevated basal levels of ppMKK1/2 were observed in the other cells lines, and treatment with U0126 resulted in a transient decrease in ppMKK1/2 levels in the BCPAP and K1 cell lines. In contrast, CI-1040 treatment had minimal effects (Fig. 4).

MKK1/2 inhibition differentially blocks the invasion of PTC and ATC cells

The effect of activated MKK1/2 signaling on the invasion of PTC and ATC cells was evaluated using Matrigel-coated transwell chambers. For these experiments, CI-1040 was used to inhibit MKK1/2 due to its higher potency, and representative images are shown in Figure 5B. The Ras-mutant C643 cells exhibited the highest rate of invasion ($\sim$500 cells/field), while the TPC1 and BCPAP cells were less invasive ($\sim$75 and 100 cells/field, respectively). The SW1736 and K1 cells were moderately invasive at 240 and 150 cells/field, respectively. After 24-hour incubation with CI-1040, the invasive capacity of the C643 cells lines was modestly reduced by 11% (Fig. 5A, $p = 0.6$). In contrast, the invasion of the TPC1 and BCPAP cells was significantly inhibited in the presence of CI-1040 (Fig. 5A, 84% and 61% inhibition, respectively, $p < 0.03$). The invasion of the SW1736 and K1 cells was inhibited by 24% and 35%, respectively, in the presence of CI-1040, but did not reach statistical significance (Fig. 5A; SW1736 $p = 0.13$; K1 $p = 0.055$). Collectively, these results indicate that MAPK signaling is critical for the invasion of the TPC1 (RET/PTC1) and BCPAP (*BRAF*) cells, while the HRAS-mutant C643, *BRAF*-mutant SW1736, and *BRAF*/PI3K-

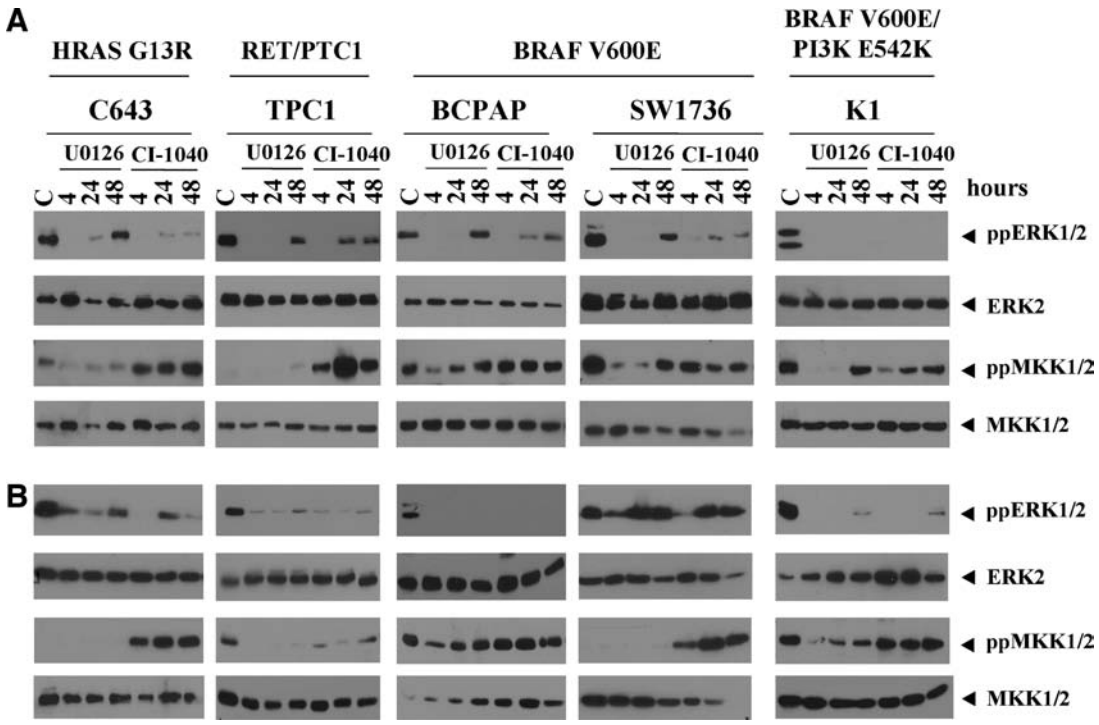

FIG. 4. Basal expression and inhibition of ppERK1/2 and ppMKK1/2 by CI-1040 or U0126 in thyroid cancer cells. C643, TPC1, BCPAP, SW1736, and K1 cells were grown in RPMI supplemented with (**A**) 10% FBS or (**B**) 2% FBS, and treated with or without the MKK1/2 inhibitors, U0126 (3 μM) or CI-1040 (0.5 μM), for the indicated times. Whole cell extracts (30 μg) were separated on 10% PAGE-SDS gels, transferred to Immobilon-P, and probed with the indicated antibodies.

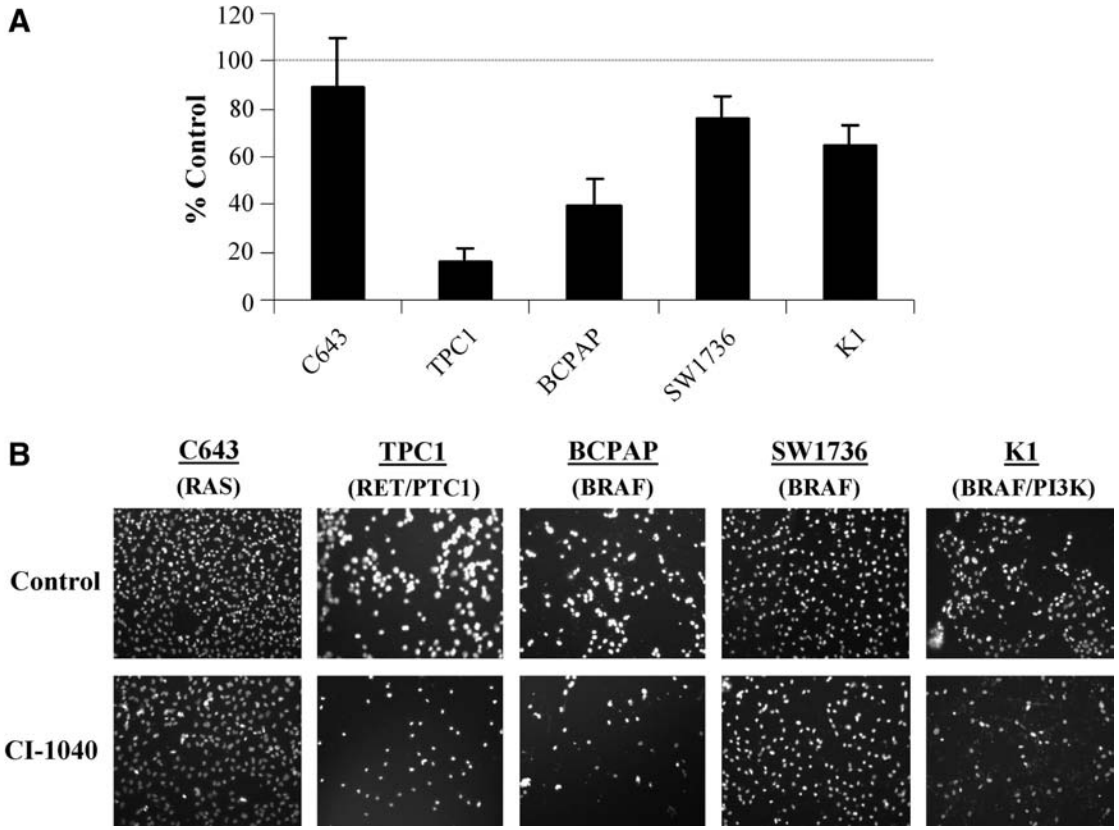

FIG. 5. The Effect of MKK1/2 inhibition on the invasion of PTC and ATC cells. (**A**) Cells were serum starved (RPMI/0.1% FBS) and pretreated $\pm 0.5\,\mu$M CI-1040 for 18 hours before plating in Matrigel-coated Boyden chambers ($8\,\mu$M pores; BD Biosciences). Cells (10^5) were allowed to invade for 24 hours toward RPMI containing 2% FBS in the presence or absence of CI-1040 ($0.5\,\mu$M). Cells on the bottom membrane were stained with DAPI, and counted using the Metamorph Imaging software. Results shown are the percentage inhibition of invading cells per field (five fields/chamber) from three independent experiments ($\pm$standard error of mean). Statistical analysis (two-tailed *t*-test) indicated that the invasion of the TPC1 and BCPAP cells was significantly inhibited by treatment with CI-1040 (TPC1 $p = 0.006$; BCPAP $p = 0.03$). (**B**) Representative images of DAPI-stained invading cells treated with or without CI-1040. DAPI, 4′,6-diamidino-2-phenylindole.

mutant K1 cell lines are less dependent on this pathway for invasion.

Characterization of PTC and ATC growth in 3D culture and inhibition of MKK1/2

Previous studies have shown that cells grown in 3D culture recapitulate tumor architecture and microenvironment found *in vivo* (32). Thus, the growth of tumor-derived cells in 3D culture represents an excellent model to study responses to potential therapeutic agents. The growth of thyroid cancer cell lines using a 3D culture overlay model has not been previously demonstrated. We therefore tested the ability of our panel of thyroid cancer cells to form spheroids in 3D culture, and representative DAPI- and Ki67-stained images are shown in Figure 6A. In 3D culture, the Ras-mutant C643 cells form branching, invasive networks, which is consistent with their high invasive potential in the Boyden chamber assay (Fig. 5B). The TPC1 (RET/PTC1) cells form disorganized solid spheroids in addition to branching structures (Fig. 6A). The *BRAF*-mutant BCPAP and *BRAF*/PI3K-mutant K1 cells form individual disorganized spheroids, and the *BRAF*-mutant SW1736 cells form disorganized solid spheroids in addition to dispersed cellular structures (Fig. 6A and data not shown). Spheroid morphology did not correlate with tumor type (ATC vs. PTC) or mutation status.

To evaluate the importance of the MAPK signaling in thyroid cancer cells grown in 3D culture, spheroids were allowed to form for 4 days and treated with or without $0.5\,\mu$M CI-1040 for the next 8 days. Growth inhibition was measured by determining average spheroid size (TPC1, BCPAP, SW1736, and K1) or average number of DAPI-positive pixels (C643). As shown in Figure 6A and B, treatment with CI-1040 resulted in a significant decrease in spheroid size in all cell lines tested. Specifically, the Ras-mutant C643 spheroids were reduced by 28% in 3D culture in the presence of CI-1040 (Fig. 6B, $p = 0.0234$). CI-1040 treatment of the TPC1 cells resulted in the abrogation of invasive structures, in addition to a reduction in average spheroid area by 55% (Fig. 6B; $p = 0.013$). The greatest reduction in spheroid size was observed in the *BRAF*-mutant cell lines: the average spheroid area of the BCPAP and K1 cells was markedly reduced by 88% and 79%, respectively (Fig. 6B; $p < 0.0001$), and the average spheroid area of the SW1736 cells was inhibited by 83% in the presence of CI-1040 (Fig. 6B; $p < 0.0001$). Thus, using 3D culture, mutational status of the MAPK pathway correlates with

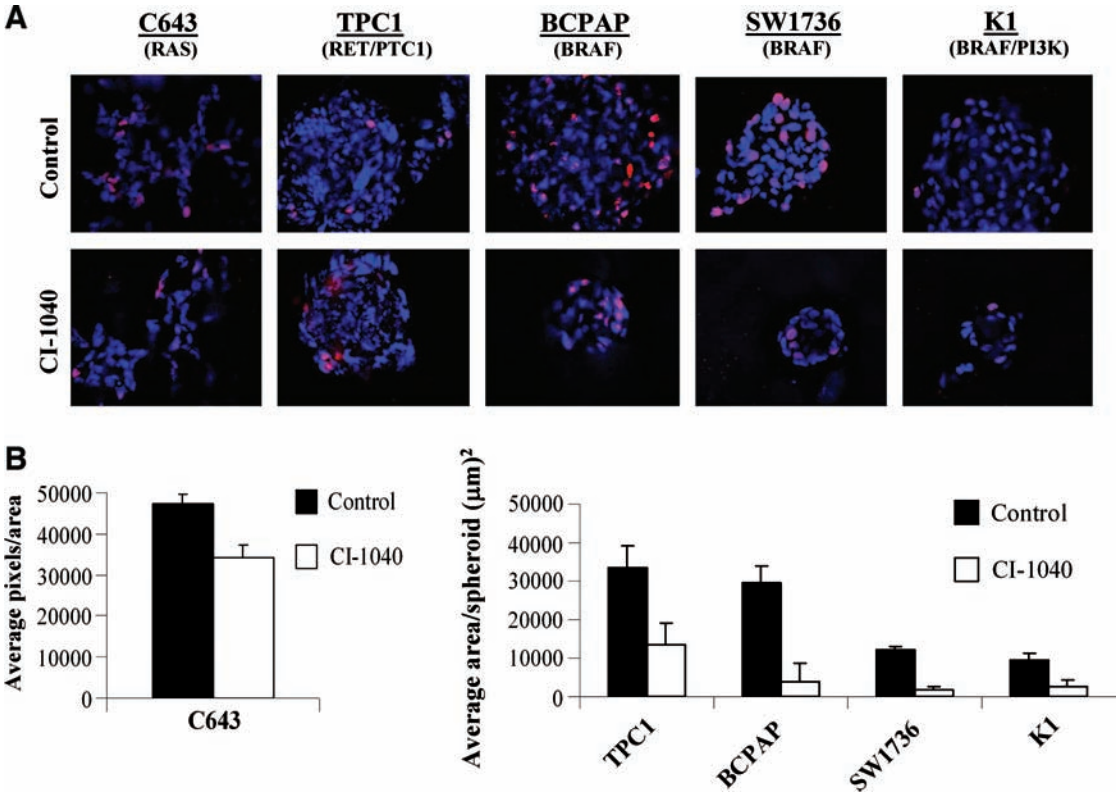

FIG. 6. Inhibition of MKK1/2 with CI-1040 differentially blocks the growth of PTC and ATC cells in three-dimensional (3D) culture. (**A**) PTC and ATC cells were grown in 3D culture for 72 hours to allow spheroid formation. Spheroids were then treated with or without 0.5 μM CI-1040 every 4 days for 8 days. Spheroids were stained with DAPI and Ki67. Representative images of three independent experiments are shown. Magnification, 40× (deconvoluted). (**B**) Quantitation of growth inhibition in 3D culture. Growth inhibition was quantitated by measuring the area $(\mu m)^2$ of spheroids in four different fields for the TPC1, BCPAP, SW1736, and K1 cells. For the C643 cells, growth inhibition was quantitated by average DAPI-positive pixel number/area in 5–7 different fields. Results presented are the mean ± standard error of mean of two replicates from one independent experiment. Statistical analysis (unpaired *t*-test) showed that CI-1040 treatment significantly reduced spheroid size (pixel number: C643 $p = 0.0234$) (spheroid size: TPC1 $p = 0.013$, BCPAP $p < 0.0001$, SW1736 $p < 0.0001$, and K1 $p < 0.0001$). Color images available online at www.liebertonline.com/thy.

MKK1/2 inhibitor sensitivity (*BRAF* > RET/PTC1 > RAS) (Fig. 6 and Table 1).

Proliferation in 3D culture was also evaluated using Ki67 staining. Figure 6A shows the presence active proliferating cells under control/untreated conditions. Treatment with CI-1040 minimally reduced Ki67 staining in the C643 cells, but resulted in a robust inhibition of proliferation in the remaining cell lines, consistent with the effect of CI-1040 treatment on cell cycle progression (Figs. 2 and 6A). No treatment completely abolished Ki67 expression at 8 days.

Discussion

The MAPK pathway plays an important role in PTC and ATC, and inhibition of this pathway may serve as a clinically relevant target. In this report, we show that the *BRAF* V600E mutation predicts sensitivity to MKK1/2 inhibition of growth; however, that other genetic alterations in the MAPK pathway (e.g., RET/PTC1) are equivalently susceptible to MKK1/2 inhibition (Table 1). Further, we show that MKK1/2 inhibition differentially inhibits the invasion of PTC and ATC cells in transwell assays independent of tumor type or proto-oncogene present (Fig. 5; Table 1), suggesting that the MAPK pathway serves distinct functions based on mutation present or tumor type.

Previous studies in melanoma have shown that growth factor signaling, in addition to oncogene-mediated signaling, is important for growth and survival (11,12). We also found that growth factors and/or mitogens present in 10% serum may diminish the effect of MKK1/2 inhibitors in 2D culture (Figs. 1 and 2). Consistent with this observation, FGFR1 signaling has been shown to play a tumor promoting role in thyroid cancer, independent of activating mutations (33), and dual inhibition of the EGF and vascular endothelial growth factor (VEGF) receptors is required to induce apoptosis and inhibit proliferation, independent of activating mutation present (34,35). Other mitogenic pathways, including c-Met and hepatocyte growth factor (HGF), also play an important role in thyroid cancer, and HGF has been shown to be a potent mitogen for thyroid follicular cells (36).

Levels of phosphorylated ERK1/2 are often used as a biomarker of response to MKK1/2 inhibitors in tumor biopsies. We attempted to correlate ppERK1/2 levels with growth inhibition and did not find a correlation between basal ppERK1/2 levels, inhibition of ppERK1/2, and growth inhibition (Figs. 1 and 4). These results are consistent with previ-

ous studies in thyroid cancer and other tumor types (4,5,24,37–40), and suggest that other markers such as Ki67, as shown for melanoma and breast cancer, may be more accurate (4,41).

A correlation between levels of phospho-MKK1/2 and sensitivity to MKK1/2 inhibitors has been previously reported in other tumor types (42,43), although some studies have found no correlation (7,40). In the studies presented here, we also did not find a strict correlation between basal ppMKK1/2 levels and sensitivity to CI-1040 or U0126 (Figs. 1 and 4), consistent with previous studies in thyroid cancer cells that used different MKK1/2 inhibitors (7). As shown in other tumor types (43–45), we also observed a paradoxical increase in ppMKK1/2 levels in response to CI-1040 or U0126 treatment (Fig. 4). Increases in ppMKK1/2 levels in response to MKK1/2 inhibitor treatment suggests that MKK1/2 inhibitors either increase or do not block MKK1/2 phosphorylation by upstream signaling cascades in some cell lines. Although we observed an accumulation of ppMKK1/2 in response to MKK1/2 inhibition in a subset of the PTC and ATC cells used in this study, we were unable to correlate the accumulation of ppMKK1/2 with *BRAF* mutational status or response to treatment, as observed in other tumor types (45). Thus, other determinants regulating sensitivity to MKK1/2 inhibitors are likely important for PTC and ATC.

Inhibition of the MAPK pathway results in an inhibition of proliferation, usually through inhibition of the G1/S restriction point of the cell cycle (3). Indeed, our results demonstrate that MAPK inhibition results in a G1-phase growth inhibition in cells harboring the *BRAF* mutation in addition to the RET/PTC1 rearrangement (Fig. 2). Our results further show that MKK1/2 inhibitors have a minimal effect on apoptosis, as measured by PARP cleavage and the lack of a sub-G1 peak by cell cycle analysis (Figs. 2 and 3). These results indicate that MKK1/2 inhibitors will likely need to be used in combination with other drugs. Previous studies have shown that MKK1/2 inhibitors sensitize cancer cells to chemotherapeutic agents and radiation therapy; thus, combinatorial approaches may represent the most promising therapeutic strategy (6,39,46).

Tetrazolium salts, such as MTS and MTT, are widely used to measure cellular proliferation and metabolism. However, several studies have reported that cell number does not always correlate with MTS/MTT assay readings (47,48). In some cases, certain drugs have been shown to increase cell size and mitochondria number, therefore influencing mitochondrial activity and reduction of formazan in the MTT assay (48,49). The precise reason for disconnect between cell number and MTS values in our current study is unclear, although a trend toward larger cell size in the CI-1040 and U0126-treated cells is intriguing (data not shown). Of note, previous studies have shown that the TPC1 cells are resistant to MKK1/2 inhibitors using the MTT assay to assess proliferation, with IC50 values ranging from $>13\,\mu$M for PD032901 to $44\,\mu$M for CI-1040 (5,50). The results from our current study indicate that the TPC1 cells are sensitive to CI-1040 ($IC50 = 0.69\,\mu$M; Fig. 1 and Table 1), as measured by ViCell cell counting, but are resistant to CI-1040 and U0126 as measured by the MTS assay (Supplemental Fig. S1). Consistent with our results, Leboeuf *et al.* also reported that the growth of the TPC1 cells is relatively sensitive to MKK1/2 inhibition ($IC50 < 100\,$nM for PD0325901 and AZD6244), as measured by ViCell counting (7). Given the potential artifacts associated with the MTS assay, we believe that cell number represents a more reliable estimate of growth and growth inhibition.

In summary, we have shown that inhibition of MKK1/2 preferentially blocks the growth of a panel of thyroid cancer cell lines harboring the *BRAF* V600E mutation, but that cells harboring distinct genetic alterations in the MAPK pathway (RET/PTC1) are also sensitive to growth inhibition. We further show that CI-1040 differentially inhibits the invasion of these thyroid cancer cell lines in a manner independent of mutational status or tumor classification. In conclusion, we show that MKK1/2 inhibitors effectively inhibit the growth of thyroid cancer cells that are dependent on the MAPK pathway, but that growth factor–mediated signaling pathways may also determine how cells will respond. MKK1/2 inhibitors may have clinical utility in patients with advanced thyroid cancer as single agent or, more likely, as combination therapy with other drugs.

Acknowledgments

We thank Dr. Andrew Bradford for critical reading of the manuscript. We also thank Vicki Van Putten for assistance with the Nikon microscope and Metamorph Imaging software, Karen Helm for assistance with the ViCell cell counter, and Steven Fadul and Clinton Cave for assistance with the Olympus spinning disk microscope. This work was supported by the American Thyroid Association and the Thyroid Head and Neck Cancer Foundation (RES), NCI K12 CA 086913 (RES), NCI CA100560 (BRH), and Mary Rossick Kern and Jerome H Kern Endowment (BRH). These studies utilized the University of Colorado Cancer Center Flow Cytometry Core supported by NIH grant P30 CA 046934.

Disclosure Statement

The authors declare that no competing financial interests exist.

References

1. Davies H, Bignell GR, Cox C, Stephens P, Edkins S, Clegg S, Teague J, Woffendin H, Garnett MJ, Bottomley W, Davis N, Dicks E, Ewing R, Floyd Y, Gray K, Hall S, Hawes R, Hughes J, Kosmidou V, Menzies A, Mould C, Parker A, Stevens C, Watt S, Hooper S, Wilson R, Jayatilake H, Gusterson BA, Cooper C, Shipley J, Hargrave D, Pritchard-Jones K, Maitland N, Chenevix-Trench G, Riggins GJ, Bigner DD, Palmieri G, Cossu A, Flanagan A, Nicholson A, Ho JW, Leung SY, Yuen ST, Weber BL, Seigler HF, Darrow TL, Paterson H, Marais R, Marshall CJ, Wooster R, Stratton MR, Futreal PA 2002 Mutations of the BRAF gene in human cancer. Nature **417:**949–954.
2. Blume-Jensen P, Hunter T 2001 Oncogenic kinase signalling. Nature **411:**355–365.
3. Sebolt-Leopold JS, Herrera R 2004 Targeting the mitogen-activated protein kinase cascade to treat cancer. Nat Rev Cancer **4:**937–947.
4. Solit DB, Garraway LA, Pratilas CA, Sawai A, Getz G, Basso A, Ye Q, Lobo JM, She Y, Osman I, Golub TR, Sebolt-Leopold J, Sellers WR, Rosen N 2006 BRAF mutation predicts sensitivity to MEK inhibition. Nature **439:** 358–362.

5. Liu D, Liu Z, Jiang D, Dackiw AP, Xing M 2007 Inhibitory effects of the MEK inhibitor CI-1040 on the proliferation and tumor growth of thyroid cancer cells with BRAF or RAS mutations. J Clin Endocrinol Metab **92:**4686–4695.
6. Yeh TC, Marsh V, Bernat BA, Ballard J, Colwell H, Evans RJ, Parry J, Smith D, Brandhuber BJ, Gross S, Marlow A, Hurley B, Lyssikatos J, Lee PA, Winkler JD, Koch K, Wallace E 2007 Biological characterization of ARRY-142886 (AZD6244), a potent, highly selective mitogen-activated protein kinase kinase 1/2 inhibitor. Clin Cancer Res **13:**1576–1583.
7. Leboeuf R, Baumgartner JE, Benezra M, Malaguarnera R, Solit D, Pratilas CA, Rosen N, Knauf JA, Fagin JA 2008 BRAFV600E mutation is associated with preferential sensitivity to MEK inhibition in thyroid cancer cell lines. J Clin Endocrinol Metab **93:**2194–2201.
8. Meier F, Busch S, Lasithiotakis K, Kulms D, Garbe C, Maczey E, Herlyn M, Schittek B 2007 Combined targeting of MAPK and AKT signalling pathways is a promising strategy for melanoma treatment. Br J Dermatol **156:**1204–1213.
9. Calipel A, Mouriaux F, Glotin AL, Malecaze F, Faussat AM, Mascarelli F 2006 Extracellular signal-regulated kinase-dependent proliferation is mediated through the protein kinase A/B-Raf pathway in human uveal melanoma cells. J Biol Chem **281:**9238–9250.
10. Gysin S, Lee SH, Dean NM, McMahon M 2005 Pharmacologic inhibition of RAF—>MEK—>ERK signaling elicits pancreatic cancer cell cycle arrest through induced expression of p27Kip1. Cancer Res **65:**4870–4880.
11. Christensen C, Guldberg P 2005 Growth factors rescue cutaneous melanoma cells from apoptosis induced by knockdown of mutated (V 600 E) B-RAF. Oncogene **24:**6292–6302.
12. Yeh AH, Bohula EA, Macaulay VM 2006 Human melanoma cells expressing V600E B-RAF are susceptible to IGF1R targeting by small interfering RNAs. Oncogene **25:**6574–6581.
13. Knauf JA, Fagin JA 2009 Role of MAPK pathway oncoproteins in thyroid cancer pathogenesis and as drug targets. Curr Opin Cell Biol **21:**296–303.
14. Xing M 2008 Recent advances in molecular biology of thyroid cancer and their clinical implications. Otolaryngol Clin North Am **41:**1135–1146, ix.
15. Ries L, Harkins D, Krapcho M, Mariotto A, Miller B, Feuer E, Clegg L, Eisner M, Horner M, Howlader N, Hayat M, Hankey B, Edwards B 2006 SEER Cancer Statistics Review, 1975–2003. National Cancer Institute, Bethesda, MD.
16. Ciampi R, Nikiforov YE 2007 RET/PTC rearrangements and BRAF mutations in thyroid tumorigenesis. Endocrinology **148:**936–941.
17. Sugg SL, Ezzat S, Zheng L, Freeman JL, Rosen IB, Asa SL 1999 Oncogene profile of papillary thyroid carcinoma. Surgery **125:**46–52.
18. Kondo T, Ezzat S, Asa SL 2006 Pathogenetic mechanisms in thyroid follicular-cell neoplasia. Nat Rev Cancer **6:**292–306.
19. Soares P, Trovisco V, Rocha AS, Feijao T, Rebocho AP, Fonseca E, Vieira de Castro I, Cameselle-Teijeiro J, Cardoso-Oliveira M, Sobrinho-Simoes M 2004 BRAF mutations typical of papillary thyroid carcinoma are more frequently detected in undifferentiated than in insular and insular-like poorly differentiated carcinomas. Virchows Arch **444:**572–576.
20. Garcia-Rostan G, Zhao H, Camp RL, Pollan M, Herrero A, Pardo J, Wu R, Carcangiu ML, Costa J, Tallini G 2003 RAS mutations are associated with aggressive tumor phenotypes and poor prognosis in thyroid cancer. J Clin Oncol **21:**3226–3235.
21. Ouyang B, Knauf J, Smith E, Zhang L, Ramsey T, Yusuff N, Batt D, Fagin J 2006 Inhibitors of Raf kinase activity block growth of thyroid cancer cells with RET/PTC or BRAF mutations *in vitro* and *in vivo*. Clin Cancer Res **12:**1785–1793.
22. Vitagliano D, Carlomagno F, Motti ML, Viglietto G, Nikiforov YE, Nikiforova MN, Hershman JM, Ryan AJ, Fusco A, Melillo RM, Santoro M 2004 Regulation of p27Kip1 protein levels contributes to mitogenic effects of the RET/PTC kinase in thyroid carcinoma cells. Cancer Res **64:**3823–3829.
23. Salvatore G, De Falco V, Salerno P, Nappi TC, Pepe S, Troncone G, Carlomagno F, Melillo RM, Wilhelm SM, Santoro M 2006 BRAF is a therapeutic target in aggressive thyroid carcinoma. Clin Cancer Res **12:**1623–1629.
24. Ball DW, Jin N, Rosen DM, Dackiw A, Sidransky D, Xing M, Nelkin BD 2007 Selective growth inhibition in BRAF mutant thyroid cancer by the mitogen-activated protein kinase kinase 1/2 inhibitor AZD6244. J Clin Endocrinol Metab **92:**4712–4718.
25. Espinosa AV, Porchia L, Ringel MD 2007 Targeting BRAF in thyroid cancer. Br J Cancer **96:**16–20.
26. Schweppe RE, Klopper JP, Korch C, Pugazhenthi U, Benezra M, Knauf JA, Fagin JA, Marlow L, Copland JA, Smallridge RC, Haugen BR 2008 Deoxyribonucleic acid profiling analysis of 40 human thyroid cancer cell lines reveals cross-contamination resulting in cell line redundancy and misidentification. J Clin Endocrinol Metab **93:**4331–4341.
27. Klopper JP, Hays WR, Sharma V, Baumbusch MA, Hershman JM, Haugen BR 2004 Retinoid X receptor-gamma and peroxisome proliferator-activated receptor-gamma expression predicts thyroid carcinoma cell response to retinoid and thiazolidinedione treatment. Mol Cancer Ther **3:**1011–1020.
28. Debnath J, Muthuswamy SK, Brugge JS 2003 Morphogenesis and oncogenesis of MCF-10A mammary epithelial acini grown in three-dimensional basement membrane cultures. Methods **30:**256–268.
29. Bain J, Plater L, Elliott M, Shpiro N, Hastie J, McLauchlan H, Klevernic I, Arthur S, Alessi D, Cohen P 2007 The selectivity of protein kinase inhibitors; a further update. Biochem J **408:**297–315.
30. Duriez PJ, Shah GM 1997 Cleavage of poly(ADP-ribose) polymerase: a sensitive parameter to study cell death. Biochem Cell Biol **75:**337–349.
31. Namba H, Nakashima M, Hayashi T, Hayashida N, Maeda S, Rogounovitch TI, Ohtsuru A, Saenko VA, Kanematsu T, Yamashita S 2003 Clinical implication of hot spot BRAF mutation, V599E, in papillary thyroid cancers. J Clin Endocrinol Metab **88:**4393–4397.
32. Smalley KS, Haass NK, Brafford PA, Lioni M, Flaherty KT, Herlyn M 2006 Multiple signaling pathways must be targeted to overcome drug resistance in cell lines derived from melanoma metastases. Mol Cancer Ther **5:**1136–1144.
33. Kondo T, Zheng L, Liu W, Kurebayashi J, Asa SL, Ezzat S 2007 Epigenetically controlled fibroblast growth factor receptor 2 signaling imposes on the RAS/BRAF/mitogen-activated protein kinase pathway to modulate thyroid cancer progression. Cancer Res **67:**5461–5470.
34. Hoffmann S, Glaser S, Wunderlich A, Lingelbach S, Dietrich C, Burchert A, Muller H, Rothmund M, Zielke A 2006 Targeting the EGF/VEGF-R system by tyrosine-kinase inhibitors—a novel antiproliferative/antiangiogenic strategy in thyroid cancer. Langenbecks Arch Surg **391:**589–596.
35. Hoffmann S, Burchert A, Wunderlich A, Wang Y, Lingelbach S, Hofbauer LC, Rothmund M, Zielke A 2007 Differ-

ential effects of cetuximab and AEE 788 on epidermal growth factor receptor (EGF-R) and vascular endothelial growth factor receptor (VEGF-R) in thyroid cancer cell lines. Endocrine **31:**105–113.
36. Bergstrom JD, Hermansson A, Diaz de Stahl T, Heldin NE 1999 Non-autocrine, constitutive activation of Met in human anaplastic thyroid carcinoma cells in culture. Br J Cancer **80:**650–656.
37. Lorusso PM, Adjei AA, Varterasian M, Gadgeel S, Reid J, Mitchell DY, Hanson L, DeLuca P, Bruzek L, Piens J, Asbury P, Van Becelaere K, Herrera R, Sebolt-Leopold J, Meyer MB 2005 Phase I and pharmacodynamic study of the oral MEK inhibitor CI-1040 in patients with advanced malignancies. J Clin Oncol **23:**5281–5293.
38. Rinehart J, Adjei AA, Lorusso PM, Waterhouse D, Hecht JR, Natale RB, Hamid O, Varterasian M, Asbury P, Kaldjian EP, Gulyas S, Mitchell DY, Herrera R, Sebolt-Leopold JS, Meyer MB 2004 Multicenter phase II study of the oral MEK inhibitor, CI-1040, in patients with advanced non-small-cell lung, breast, colon, and pancreatic cancer. J Clin Oncol **22:**4456–4462.
39. Haass NK, Sproesser K, Nguyen TK, Contractor R, Medina CA, Nathanson KL, Herlyn M, Smalley KS 2008 The mitogen-activated protein/extracellular signal-regulated kinase kinase inhibitor AZD6244 (ARRY-142886) induces growth arrest in melanoma cells and tumor regression when combined with docetaxel. Clin Cancer Res **14:**230–239.
40. Wang YF, Jiang CC, Kiejda KA, Gillespie S, Zhang XD, Hersey P 2007 Apoptosis induction in human melanoma cells by inhibition of MEK is caspase-independent and mediated by the Bcl-2 family members PUMA, Bim, and Mcl-1. Clin Cancer Res **13:**4934–4942.
41. Smalley KS, Contractor R, Haass NK, Lee JT, Nathanson KL, Medina CA, Flaherty KT, Herlyn M 2007 Ki67 expression levels are a better marker of reduced melanoma growth following MEK inhibitor treatment than phospho-ERK levels. Br J Cancer **96:**445–449.
42. Abi-Habib RJ, Urieto JO, Liu S, Leppla SH, Duesbery NS, Frankel AE 2005 BRAF status and mitogen-activated protein/extracellular signal-regulated kinase kinase 1/2 activity indicate sensitivity of melanoma cells to anthrax lethal toxin. Mol Cancer Ther **4:**1303–1310.
43. Huynh H, Soo KC, Chow PK, Tran E 2007 Targeted inhibition of the extracellular signal-regulated kinase kinase pathway with AZD6244 (ARRY-142886) in the treatment of hepatocellular carcinoma. Mol Cancer Ther **6:**138–146.
44. Ahn N, Stines Nahreini T, Tolwinski N, Resing K 2001 Pharmacologic inhibitors of MKK1 and MKK2. Methods Enzymol **332:**417–431.
45. Friday BB, Yu C, Dy GK, Smith PD, Wang L, Thibodeau SN, Adjei AA 2008 BRAF V600E disrupts AZD6244-induced abrogation of negative feedback pathways between extracellular signal-regulated kinase and Raf proteins. Cancer Res **68:**6145–6153.
46. Qiao L, Yacoub A, McKinstry R, Park JS, Caron R, Fisher PB, Hagan MP, Grant S, Dent P 2002 Pharmocologic inhibitors of the mitogen activated protein kinase cascade have the potential to interact with ionizing radiation exposure to induce cell death in carcinoma cells by multiple mechanisms. Cancer Biol Ther **1:**168–176.
47. Huang KT, Chen YH, Walker AM 2004 Inaccuracies in MTS assays: major distorting effects of medium, serum albumin, and fatty acids. Biotechniques **37:**406, 408, 410–402.
48. Pagliacci MC, Spinozzi F, Migliorati G, Fumi G, Smacchia M, Grignani F, Riccardi C, Nicoletti I 1993 Genistein inhibits tumour cell growth *in vitro* but enhances mitochondrial reduction of tetrazolium salts: a further pitfall in the use of the MTT assay for evaluating cell growth and survival. Eur J Cancer **29A:**1573–1577.
49. Sobottka SB, Berger MR 1992 Assessment of antineoplastic agents by MTT assay: partial underestimation of antiproliferative properties. Cancer Chemother Pharmacol **30:** 385–393.
50. Liu D, Xing M 2008 Potent inhibition of thyroid cancer cells by the MEK inhibitor PD0325901 and its potentiation by suppression of the PI3K and NF-kappaB pathways. Thyroid **18:**853–864.

Address correspondence to:
Rebecca E. Schweppe, Ph.D.
Division of Endocrinology, Diabetes, and Metabolism
University of Colorado Denver
12801 E 17th Ave., MS 8106
P.O. Box 6511
Aurora, CO 80045

E-mail: rebecca.schweppe@ucdenver.edu